

Orbital density wave order and electronic correlation driven insulating 1T-TaS₂ monolayer

Xiang-Long Yu¹, Da-Yong Liu¹, H.-Q. Lin², Ting Jia¹, and Liang-Jian Zou^{1,3*}

¹ Key Laboratory of Materials Physics, Institute of Solid State Physics,
Chinese Academy of Sciences, P. O. Box 1129, Hefei 230031, China

² Beijing Computational Science Research Center, Beijing 100084, China and

³ Department of Physics, University of Science and Technology of China, Hefei 230026, China

(Dated: October 2, 2018)

We present the orbital resolved electronic properties of structurally distorted 1T-TaS₂ monolayers. After optimizing the crystal structures, we obtain the lattice parameters and atomic positions in the star-of-David structure, and show the low-temperature band structures of distorted bulk are consistent with recent angle resolved photoemission spectroscopy (ARPES) data. We further clearly demonstrate that 5d electrons of Ta form ordered orbital-density-wave (ODW) state with dominant $5d_{3z^2-r^2}$ character in central Ta, driving the one-dimensional metallic state in paramagnetic bulk and half-filled insulator in monolayer. Meanwhile, the star-of-David distortion in monolayers favors charge density wave and the flat band stabilizes ferromagnetic density wave of Ta spins with the same wavevector of ODW $\frac{4}{13}\mathbf{b}_1 + \frac{1}{13}\mathbf{b}_2$. We propose that 1T-TaS₂ monolayer may pave a new way to study the exciton physics, exciton-polaron coupling, and potential applications for its exciton luminescence.

Layered transition-metal dichalcogenide 1T-TaS₂ not only undergoes several complicated charge-density-wave (CDW) phase transitions with decreasing temperature, but also exhibits marvelous metal-insulator transition when temperature further decreases to enough low T, and even becomes superconducting upon doping¹ or under high pressure^{2,3}. To account for the nature of the low-T insulating phase in CDW ordered bulk 1T-TaS₂, the Mott insulator mechanism induced by electron-electron correlation^{1,4-6} and the CDW insulator mechanism arising from the electron-phonon coupling or Fermi surface nesting⁷⁻⁹ were proposed and have been debated more than thirty years. Early argument that low-T 1T-TaS₂ is a Mott insulator was based on the fact that a half-filled band crosses the Fermi energy and the low-T resistivity diverges, thus the electronic correlation in 1T-TaS₂ was believed to play crucial role in 1T-TaS₂ in the low-T insulating regime of T < 180K^{4,5}. However, the typical characters of Mott insulator were not well confirmed experimentally until now: lower and upper Hubbard bands and Mott insulating gap in optical spectra and conductivity, magnetic moment and Curie-Weiss susceptibility in neutron scattering and other magnetic experiments. Recent years the interest to nature of low-T phase in 1T-TaS₂ has revived¹⁰⁻¹² to examine the concept of Mott physics in distorted CDW phase, and tried to find more clues in electronic states to confirm the role of electronic correlation in the low-T insulating 1T-TaS₂.

On the other hand, with the discovery of graphene, many experimentalists are trying to exfoliate many layered/quasi-two-dimensional compounds, including transition-metal dichalcogenides in order to find more monolayer systems, and explore their unusual properties of these monolayer compounds/two-dimensional electron systems¹³. One of recent successful examples is the monolayer molybdenum dichalcogenides MoS₂, in which Mo ions also form a 2-dimensional hexagonal lattice, similar to graphene. Despite of great works on two-dimensional MoS₂, the lack of high-quality 1T-TaS₂ sample hampers the study on monolayer 1T-TaS₂. Very recently, Chen *et al.* successfully exfoliated 1T-TaS₂ thin films of a few atomic layers experimentally, and observed a clear transition from a metal to an insulator

when the bulk reduces to several atomic layers, and the CDW hysteresis gradually vanishes one by one when the thickness of the thin film reduces to about 3 atomic layers¹⁴. Meanwhile, Darancet *et al.*¹² showed that 1T-TaS₂ monolayer may be an Mott insulator with a half-filled flat band. These experimental and theoretical explorations may not only pave a new way to study novel properties of 1T-TaS₂ monolayer with CDW state and Mott physics, but also provide the possible applications of transition-metal dichalcogenides in electronic devices and sensors.

In this Letter, we unambiguously demonstrate that the ground state of 1T-TaS₂ monolayer in optimized distorted structure forms orbital order or orbital density wave (ODW) states with the wavevector $\frac{4}{13}\mathbf{b}_1 + \frac{1}{13}\mathbf{b}_2$ in monolayer 1T-TaS₂. In this scenario, the central Ta has dominant $5d_{3z^2-r^2}$ orbital component, and orbital polarization gradually decays from the central Ta of star-of-David to outer-ring Ta, we also predict the ferromagnetic spin density wave state and distribution of Ta magnetic moments, in consistent with the ODW in the distorted crystal structures. We could also present the band structures of monolayer and few-layer thin films, and point out that our calculated band structures agree with recent angle resolved photoemission spectra (ARPES) data in distorted bulk. Such an ODW scenario could interpret not only the quasi-one-dimensional metallic ground state in bulk 1T-TaS₂, but also predict the MIT when the system reduces to multilayer thin film, and monolayer. We suggest that both the Coulomb correlation and electron-phonon coupling play key roles.

We firstly perform the structural optimizations of 1T-TaS₂ including monolayer, and bulk both in the low-temperature phase with lattice distortion and in the high-temperature phase without distortion. We find that comparing with 1T-TaS₂ bulk, the radius of star-of-David and the Ta-Ta distance in monolayer slightly expand less than 0.3%; on the other hand, the Ta-S distance slightly shrinks, no more than 0.3%. From these optimized structures one obtains the basic features of the electronic structure in high-symmetry normal phase and low-temperature distorted phase through performing the generalized gradient approximation (GGA) calculations and its correlation correction (GGA+U) for 1T-TaS₂ bulk and mono-

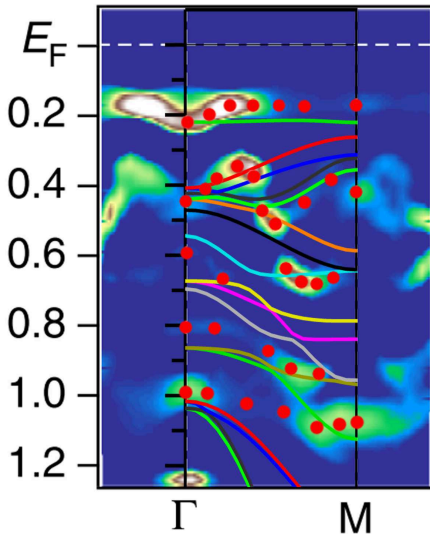


FIG. 1: (Color online) Comparison of bulk CCDW-state energy bands between our results with the correlation correction of $U = 2$ eV and ARPES experiment by Ang *et al.*¹¹. Red points are artificially to highlight occupied states in ARPES, and the curves are the energy bands obtained by our first-principles calculations.

layer. The details of numerical calculations could be seen in the *Supplementary Materials*.

The low-T distorted superstructure phase of bulk 1T-TaS₂ is a commensurate charge density wave (CCDW) state below 180 K, and is characterized by star-shaped clusters of 13 atoms in the Ta plane¹. The electronic band structures of bulk 1T-TaS₂ without correlation correction in the CCDW phase show that each star-of-David unit cell hosts one half-filled band crossing the Fermi level with the energy bandwidth about 0.4 eV, and this band displays a rather weak in-plane dispersion but a strong out-of-plane one, indicating a one-dimensional metal for bulk. Also there are a few bands from -0.2 eV to -1 eV where only one or two bands are involved in high-T phase. Moreover, with consideration of correlation correction, an interlayer-antiferromagnetic ground state is obtained, and the half-filled band splits into upper and lower Hubbard bands. These theoretical results are consistent with the available angle resolved photoemission spectroscopy (ARPES) data, despite of dispersed results in the ARPES experiments on the band structure and Fermi surface in the CCDW phase around the Γ point^{11,15–17}. Comparing the details of our band structures with $U = 2$ eV to recent ARPES results measured at 30 K by Ang *et al.* along $\Gamma - M$ ¹¹, as shown in Fig. 1, we find their global agreement in the energy range from E_f to -1 eV: near -0.2 eV, both experiment and calculation results show flat dispersion and the maximum energy difference is about 0.05 eV. Below -0.2 eV, the momentum dependence of each band is in substantial agreement with the ARPES data. In particular, considering rough bands degeneracy, our six bands around Γ point agree with Pillo *et al.*'s observation of the existence of at least six different CDW-induced peaks¹⁶.

Due to weak van der Waals interaction between TaS₂ layers,

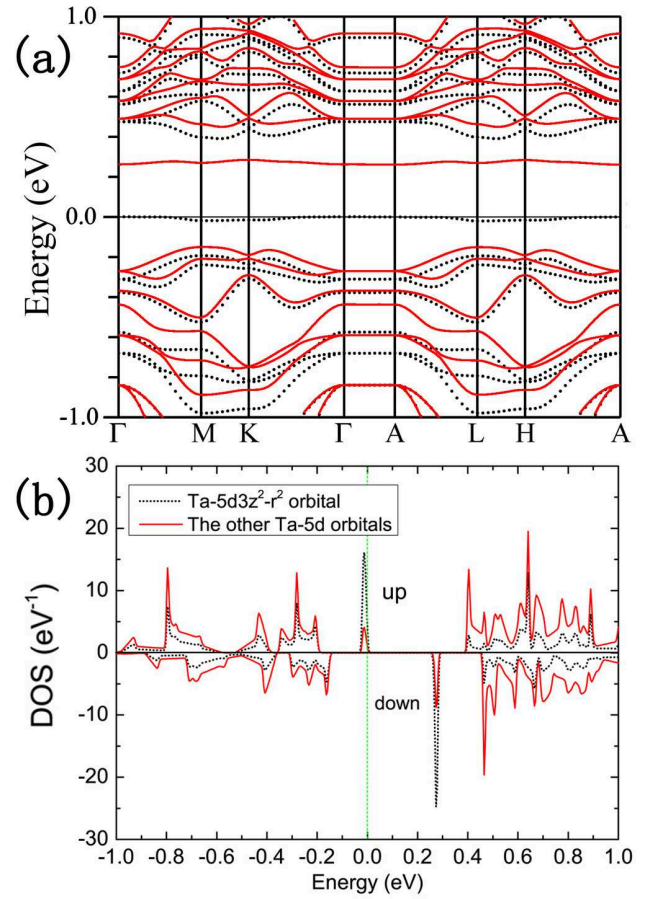


FIG. 2: (Color online) Band structures (a) and orbital resolved density of states (b) for distorted monolayer 1T-TaS₂ in the GGA + U scheme. Theoretical parameter $U = 2$ eV.

similar to graphene and MoS₂, one may exfoliate a few layers 1T-TaS₂, or even monolayer from a bulk. For a 1T-TaS₂ monolayer, after optimizing its lattice structure and atomic positions, our GGA calculation shows that a very narrow energy band with the bandwidth of less than 20 meV lies on the Fermi level E_f . The evolution of such a flat band on E_f with increasing distortion could be seen in the *Supplementary Materials*. The broken of the translation invariance in the c -axis in the monolayer leads to the vanish of the dispersion along $\Gamma - A$ direction, leaving a half-filled narrow band with significant contribution of Ta- $5d_{3z^2-r^2}$ orbital. After taking into account the correlation correction in the GGA+ U calculation with $U = 2$ eV, the half-filled flat band on E_f splits into empty upper Hubbard band and a full-filled lower Hubbard band, opening a gap of ~ 0.25 eV, as shown in Fig. 2 (a). Further the DOS in Fig. 2 b displays that the orbital symmetry character of DOS around E_f are major Ta $5d_{3z^2-r^2}$, and the ground state of 1T-TaS₂ monolayer is orbital and spin polarized.

In 1T-TaS₂, due to the trigonal crystalline field of S ions on Ta ions in TaS₆ octahedra, the active orbitals of Ta 5d electrons are three t_{2g} components $d_{3z^2-r^2}$, e_{g1} and e_{g2} , which are the

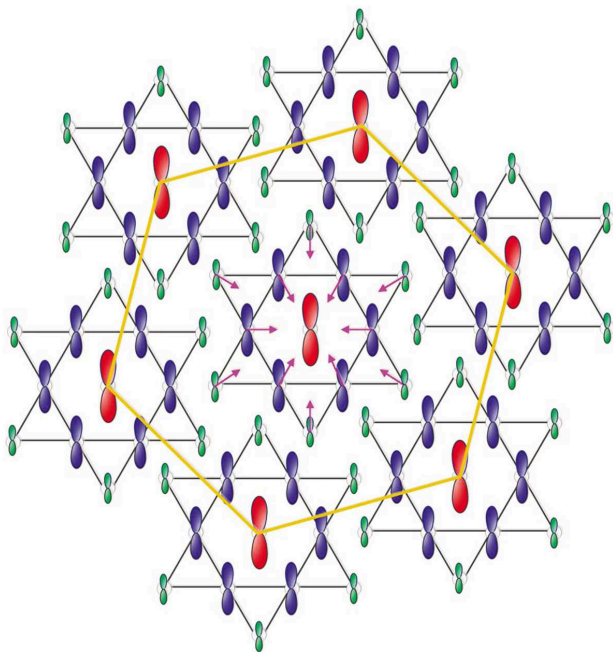


FIG. 3: (Color online) Schematic diagram of the orbital density wave order in a star of Ta lattice in 1T-TaS₂ monolayer. Arrows indicate the distortion direction of Ta atoms. Ferromagnetic spin density wave shares the same period.

recombination of three orbital components d_{XY} , d_{YZ} and d_{XZ} (here X, Y, and Z are the variables in the original global coordinate system) in accordance with the trigonal crystalline field symmetry. The orbital character of the energy band around the Fermi level is also analyzed quantitatively, and the orbital weights are summarized in Table I. Ta $5d_{3z^2-r^2}$ orbital contributes significantly at E_F , especially the one of Ta atoms in the interior of the star. The weights of the other four 5d orbitals are nearly negligible. Such an orbital feature not only address the unique dispersion in the ab -plane, but also is consistent with the one-dimensional metallicity along c direction in bulk 1T-TaS₂. It is thus naturally expected that the metal-insulator transition occurs when the bulk reduces to a monolayer. It is worth noting that the weight of the $5d_{3z^2-r^2}$ orbital decreases gradually from the center to the edge in the Ta star, forming an ODW. This unusual behavior origins from the star-of-David distortion. Besides the inward contraction of Ta atoms, the out-of-plane buckling of S atoms also plays an important role.

Fig. 3 is a schematic diagram of the atomic position and orbital distribution in a star: the Ta-Ta distance of the internal ring is shorter than that of outer ring so that Ta-S-Ta angle is small and height of Ta-S is large, which is in favor of a hybridization between Ta- $5d$ and S- $4p_z$ orbital and contributes major $5d_{3z^2-r^2}$ orbital component; as a contrast, in the outer ring of stars long distance between two Ta atoms, large Ta-S-Ta angle and short vertical height of Ta-S atoms lead to a weakened hybridization of Ta- $5d$ and S- $4p_z$ orbitals, while an enhanced Ta- $5d$ and S- $4p_{x/y}$ hybridization; thus from the center to the edge of star, the $5d_{3z^2-r^2}$ orbital polarization grad-

ually reduces; therefore, the orbital polarization is upmost in the center of star, and minimum in the edge, forming a ferro-orbital density wave order over the whole monolayer. The distribution of orbital polarization in a Ta star is summarized in Table I. One anticipates that in a bulk such an orbital order scenario also validates.

It is interesting that whether CDW order remains exist in 1T-TaS₂ monolayer. From our optimized lattice one notices that the lattice distortion in monolayer is still significant and has a little difference from the CCDW phase in bulk. However, a very recent experiment by Chen *et al.*¹⁴ showed that the thermal hysteresis in resistivity indicating the pinning of CDW greatly weakens and even disappears once 1T-TaS₂ bulk reduces to a few layers. The Ta plane shown in Fig. 3 illustrates the CDW-induced displacements that lead to the commensurate $\sqrt{13} \times \sqrt{13} - R13.9^\circ$ superlattice, similar to observed in the low-temperature phase of bulk^{3,18,19}. The corresponding lattice vectors of the superlattice with respect to that in high-temperature homogeneous phase are $\mathbf{R}_1 = 3\mathbf{a}_1 + \mathbf{a}_2$, $\mathbf{R}_2 = -\mathbf{a}_1 + 4\mathbf{a}_2$.

To indicate the role of electronically driven instabilities as the origin of the star-of-David distortion in the ground state, we have also analyzed the Fermi surface nesting in high-temperature homogeneous phase and calculated the static electronic susceptibility χ , which is defined as

$$\chi(\mathbf{q}) = \frac{1}{N} \sum_{k,m,n} \frac{f(\varepsilon_n(\mathbf{k})) [1 - f(\varepsilon_m(\mathbf{k} + \mathbf{q}))]}{\varepsilon_m(\mathbf{k} + \mathbf{q}) - \varepsilon_n(\mathbf{k}) + i\eta}. \quad (1)$$

Here $\varepsilon_m(\mathbf{k})$ is the quasiparticle spectrum of the energy band m obtained from the first-principles calculations by the GGA method, from which one may get insight to the charge and magnetic instability of monolayer 1T-TaS₂. The electronic susceptibility in 1T-TaS₂ monolayer shown in Fig. 4 indicates a sharp peak, corresponding to a divergence, implying that the Fermi surface nesting of the monolayer is perfect. The global maximum of the electronic susceptibility appears around $0.295\mathbf{b}_1$, corresponding to a nesting vector. However, through further analysis, we find the calculated nesting vectors and the star-of-David displacements do not match very well. As shown above, the electronic susceptibility displays two similar but independent nesting vectors $\mathbf{Q}_1 = 0.295\mathbf{b}_1$ and $\mathbf{Q}_2 = 0.295\mathbf{b}_2$, respectively. A possible spin and charge density waves may oscillate as $\cos(\mathbf{Q} \cdot \mathbf{R})$ on the Ta plane, with a wave vector \mathbf{Q} . This vector is equal to a commensurate linear combination of \mathbf{Q}_1 and \mathbf{Q}_2 , namely $\mathbf{Q} = x\mathbf{Q}_1 + y\mathbf{Q}_2$. Through detailed calculations, a wave vector $\mathbf{Q} = \frac{4}{13}\mathbf{b}_1 + \frac{1}{13}\mathbf{b}_2$ is determined with $x = 1.043$ and $y = 0.261$, consistent with the star-of-David distortion^{3,19,20}.

As a strong e-ph-coupling Mott insulator, the magnetic properties of 1T-TaS₂ bulk remains an unsettled problem. Earlier data showed that CCDW bulk is paramagnetic^{1,4,5}, whereas, recent experiments suggested a strong layered ferromagnetic order²¹. Revealing the magnetism of 1T-TaS₂ monolayer not only favors but also is useful for our understanding the magnetism of 1T-TaS₂ bulk. Our correlation correction calculation in the GGA+ U scheme shows that magnetic moment is mainly contributed from the central and first-ring

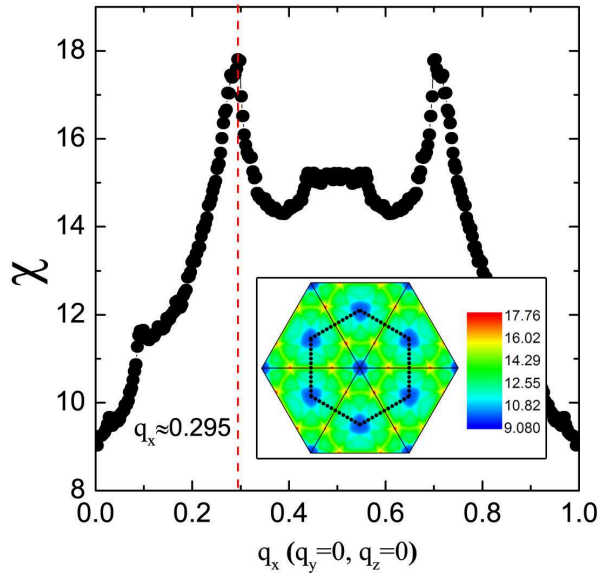


FIG. 4: (Color online) Real part of static electronic susceptibility with arbitrary unit ν vs wavevector along $\Gamma - M$ direction. Inset shows its distribution in momentum space. The dotted line frame corresponds to the first Brillouin zone of the monolayer in high-temperature normal phase.

Ta $5d_{3z^2-r^2}$ orbitals of the star cluster. The energy gap opening causes a nonuniform distribution of magnetic moment in the star cluster where the magnetic moments per Ta atom for the central, first-ring and second-ring Ta are 0.272 , 0.04 and $0.01\mu_B$, respectively, demonstrating that the ground state of a monolayer 1T-TaS₂ is ferromagnetic density wave ordered. The distribution of magnetic moments of Ta in a star-of-David is also summarized in Table I.

For an intuitive picture of the CCDW phase, the charge density has been calculated with cutoff energy $-1Ry$ to truncate the contribution from atomic core. Fig. 5 displays the charge density of Ta-atom cross section. One can find that every 13 Ta atoms form a star-of-David cluster with a perfect six-fold symmetry, and the charge density of the interval regime between two clusters is small, just like a moat which leads to an in-plane insulator. This is also consistent with our preceding band analysis. These interesting and unusual behaviors of 1T-TaS₂ monolayer all originate from the formation of the star-of-David distortion and the ODW order.

We have shown that orbital physics plays a key role in the $5d$ 1T-TaS₂ monolayer, as well as bulk. Though on-site Coulomb interaction may be necessary and the Mott localization may happen in two-dimensional monolayer, such as TiS₂ and VS₂, we attribute the origin of the orbital density wave mainly to strong e-ph coupling in 1T-TaS₂, since we find that sufficient large Coulomb correlation U could not drive the high-T undistorted phase of a monolayer from metal to insulator, implying the e-ph coupling driven Jahn-Teller-like distortion establish predominant $5d_{3z^2-r^2}$ orbital component and the ferro-orbital density wave order from a undistorted three-orbital system. Therefore when a 1T-TaS₂ bulk reduces to a few layers or even monolayer, conduction electrons in $d_{3z^2-r^2}$

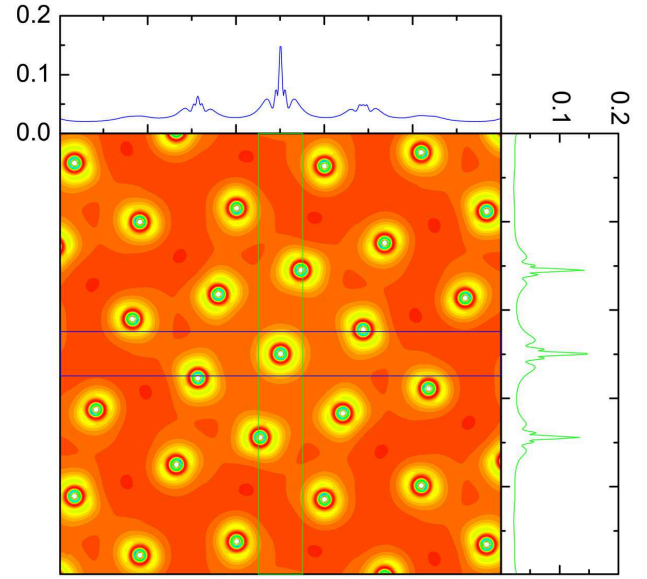


FIG. 5: (Color online) Charge density distribution of Ta-atom cross section in distorted monolayer 1T-TaS₂. The top blue and right green lines correspond to the charge density in the blue and green boxes, respectively.

orbital become discrete and localized. The Coulomb interaction and e-ph coupling drive the ferromagnetic and charge density waves in the monolayer with the same wavevector of the orbital order.

From our study for various situations we find that the LS coupling do not play considerable roles on the ground state. This is a resultant of the orbital order in TaS₂ monolayer. Since the Ta $5d$ electrons predominately occupy $d_{3z^2-r^2}$ orbit near the Fermi level, forming an effective single orbital system. Therefore the LS coupling plays little role on the groundstate electronic properties on 1T-TaS₂ monolayer and bulk, though its coupling strength is considerable. It is also worthy of stressing that the the orbital properties of bulk 1T-TaS₂ are expected to similar to the present orbital character of monolayer, as seen the *Supplementary Materials*.

One may notice that 1T-TaS₂ is a strongly coupled e-ph interacting system²², we anticipate that the electron-phonon interaction may play considerable roles not only in the star-of-David distortion, but also in transport in monolayer, as the polaronic effect in dynamic process of bulk²⁰. The successful synthesis of 1T-TaS₂ monolayer may pave a new way to study the novel properties of 1T-TaS₂ monolayer with CDW state and Mott physics; its flat band character and insulating gap could lead to exciton-polaron coupling, exciton luminescence and dynamical properties, which may provide the possible applications of transition-metal dichalcogenides in electronic devices and sensors.

The authors acknowledge X. H. Chen for providing primary experimental data. This work was supported by the National Science Foundation of China under Grant no. 11274310 and 11104274, and the Hefei Center for Physical Science and Technology under Grant no. 2012FXZY004. Numerical cal-

culations were performed at the Center for Computational Science of CASHIPS.

- * Corresponding author. E-mail: zou@theory.issp.ac.cn
- ¹ J. A. Wilson, F. J. Di Salvo, and S. Mahajan, *Adv. Phys.* **24**, 117 (1975).
- ² T. Ritschel, J. Trinckauf, G. Garbarino, M. Hanfland, M. v. Zimmermann, H. Berger, B. Büchner, and J. Geck, *Phys. Rev. B* **87**, 125135 (2013).
- ³ B. Sipos, A. F. Kusmartseva, A. Akrap, H. Berger, L. Forró, and E. Tutiš, *Nature Mater.* **7**, 960 (2008).
- ⁴ P. Fazekas, and E. Tosatti, *Philo. Mag. B* **39**, 229 (1979).
- ⁵ P. Fazekas, and E. Tosatti, *Physica B+C* **99**, 183 (1980).
- ⁶ P. A. Lee, and T. V. Ramekrishnan, *Rev. Mod. Phys.* **57**, 287 (1985).
- ⁷ F. J. Di Salvo, J. A. Wilson, B. G. Bagley, and J. V. Waszczak, *Phys. Rev. B* **12**, 2220 (1975).
- ⁸ R. Imamda, Y. Onuki, and S. Tanuma, *Physica B* **99**, 188 (1980).
- ⁹ B. Dardel, M. Grioni, D. Malterre, P. Weibel, Y. Baer, and F. Lévy, *Phys. Rev. B* **45**, 1462(R) (1992).
- ¹⁰ B. Sipos, A. F. Kusmartseva, A. Akrap, H. Berger, L. Forró, and E. Tutiš, *Nature Mater.* **7**, 2318 (2008).
- ¹¹ R. Ang, Y. Tanaka, E. Ieki, K. Nakayama, T. Sato, L. J. Li, W. J. Lu, Y. P. Sun, and T. Takahashi, *Phys. Rev. Lett.* **109**, 176403 (2012).
- ¹² P. Darancet, A. J. Millis, and C. A. Marianetti, arXiv: 1401.0246 (2014).
- ¹³ K.S. Novoselov, D. Jiang, F. Schedin, T. J. Booth, V. V. Khotkevich, S. V. Morozov, and A. K. Geim, *Proc. Nat. Acad. Soc.* **102**, 10451 (2005).
- ¹⁴ Y. B. Zhang and X. H. Chen, private communication (2014).
- ¹⁵ F. Zwick, H. Berger, I. Vobornik, G. Margaritondo, L. Forró, C. Beeli, M. Onellion, G. Panaccione, A. Taleb-Ibrahimi, and M. Grioni, *Phys. Rev. Lett.* **81**, 1058 (1998).
- ¹⁶ Th. Pillo, J. Hayoz, D. Naumović, H. Berger, L. Perfetti, L. Gavioli, A. Taleb-Ibrahimi, L. Schlapbach, and P. Aebi, *Phys. Rev. B* **64**, 245105 (2001).
- ¹⁷ J. C. Petersen, S. Kaiser, N. Dean, A. Simoncig, H. Y. Liu, A. L. Cavalieri, C. Cacho, I. C. E. Turcu, E. Springate, F. Frassetto, L. Poletto, S. S. Dhesi, H. Berger, and A. Cavalleri, *Phys. Rev. Lett.* **107**, 177402 (2011).
- ¹⁸ K. Nakanishi, and H. Shiba, *J. Phys. Soc. Jpn.* **53**, 1103 (1984).
- ¹⁹ C. B. Scruby, P. M. Williams, and G. S. Parry, *Phil. Mag.* **31**, 255 (1975).
- ²⁰ L. Stojchevska, I. Vaskivskiy, T. Mertelj, P. Kusar, D. Svetin, S. Brazovskii, and D. Mihailovic, *Science*, **344**, 177 (2014).
- ²¹ L. Perfetti, T. A. Gloor, F. Mila, H. Berger, and M. Grioni, *Phys. Rev. B* **71**, 153101 (2005).
- ²² K. Rossnagel, *J. Phys. Conden. Matt.* **23**, 213001 (2011).

TABLE I: Orbital resolved character of a Ta star-of-David in distorted monolayer 1T-TaS₂.

	13 Ta atoms	26 S atoms	Interstitial electrons	
Atomic weight	0.47925	0.18420	0.33654	
Central atom	1 Ta	5 <i>d</i> orbital	5 <i>d</i> _{3z²-r²} orbital	Other 5 <i>d</i> orbitals
Orbital weight	0.14125	0.14090	0.13917	0.00174
First-ring atoms	6 Ta	5 <i>d</i> orbital	5 <i>d</i> _{3z²-r²} orbital	Other 5 <i>d</i> orbitals
Orbital weight	0.24214	0.03983	0.03667	0.00316
Second-ring atoms	6 Ta	5 <i>d</i> orbital	5 <i>d</i> _{3z²-r²} orbital	Other 5 <i>d</i> orbitals
Orbital weight	0.09587	0.01581	0.00174	0.01407